I&EC research
Industrial & Engineering Chemistry Research

Review

pubs.acs.org/IECR

Enhanced Charge Separation in Nanostructured TiO_2 Materials for Photocatalytic and Photovoltaic Applications

He He, Chao Liu, Kevin D. Dubois, Tong Jin, Michael E. Louis, and Gonghu Li*

Department of Chemistry and Materials Science Program, University of New Hampshire, Durham, New Hampshire 03824, United States

ABSTRACT: Titanium dioxide (TiO_2) has been extensively investigated in solar energy applications, including heterogeneous photocatalysis and photovoltaics. For most TiO_2 materials, charge recombination between photoexcited electrons and holes severely limits the efficiencies of solar energy conversion. Different strategies have been attempted to improve charge separation in TiO_2 materials. This review focuses on three effective approaches to achieve enhanced charge separation by constructing mixed-phase TiO_2, highly dispersed titanium oxides, and nanotubular TiO_2 materials. Selected examples from the literature are discussed to demonstrate how the three approaches could be implemented in the context of photocatalytic water splitting, photocatalytic CO_2 reduction, and dye-sensitized solar cells. The discussion provides useful insights regarding the design of new TiO_2 nanostructures for use in solar energy conversion.

1. INTRODUCTION

As a wide bandgap semiconductor, titanium dioxide (TiO_2) is inexpensive, chemically and biologically nontoxic, and robust under photochemical conditions.[1,2] Nanostructured TiO_2 materials have been extensively investigated in photocatalytic and photovoltaic applications. The principles of TiO_2 photocatalysis are described in several review articles.[3−8] Upon photoactivation, electrons (e^-) in TiO_2 valence band (VB) can be excited into the conduction band (CB), leaving behind positively charged holes (h^+, Figure 1). In the absence of charge traps or scavengers, recombination occurs between the CB electrons and VB holes. When charge recombination occurs, the photonic energy dissipates as heat and no chemical transformation happens. In photocatalysis, the electrons and/or holes diffuse to the surface and participate in chemical reactions, converting photonic energy into chemical energy.

A major limitation of TiO_2 materials is the low efficiency in most photocatalytic processes due to electron−hole recombination which prevails in the bulk. Different strategies have been studied in order to improve charge separation in TiO_2 photocatalysis by modifying surface and/or bulk structures as well as forming nanocomposites.[9−11] For example, spatial charge separation can be achieved in metal−semiconductor composites such as Pt/TiO_2, in which the metal nanoparticles function as electrons sinks to hinder charge recombination. This article focuses on three types of nanostructures that have shown enhanced charge separation, including mixed-phase TiO_2, highly dispersed titanium oxides, and TiO_2 nanotubes. Specific examples will be discussed regarding how the three types of nanostructures lead to improved performance in photocatalytic water splitting, photocatalytic CO_2 reduction, and dye-sensitized solar cells.

2. SOLAR ENERGY CONVERSION USING TiO_2 MATERIALS

The early work by Fujishima, Honda, and co-workers demonstrated that TiO_2 materials are promising photocatalysts for solar fuel production by water splitting[12] and CO_2 reduction.[13] As shown in Figure 1a, the band structure of TiO_2 brackets the redox potential for water splitting, suggesting that the photoexcited electrons in TiO_2 CB are able to reduce protons into hydrogen and the VB holes are capable of oxidizing H_2O into oxygen (Reactions 1 and 2, potentials versus NHE at pH 7). In fact, TiO_2 materials have been exploited as heterogeneous photocatalysts for H_2 generation via water splitting.[14] The energy diagram shown in Figure 1b indicates that the electrons in TiO_2 CB are able to reduce CO_2 into CH_3OH and CH_4.[15−18] Therefore, activated TiO_2 materials could also catalyze CO_2 reduction via proton-coupled pathways (Reactions 3 and 4, potentials versus NHE at pH 7)[19,20] in the presence of appropriate electron donors such as isopropanol. Water could serve as a renewable electron donor in TiO_2-catalyzed CO_2 reduction because photoexcited holes in TiO_2 VB are energetic enough for water oxidation (Reaction 2). However, the reaction between CO_2 and H_2O proceeds with very low efficiency on TiO_2 surfaces because the individual half reactions (Reactions 2, 3, and 4) require the accumulation of multiple redox equivalents, which is extremely difficult because of the prevailing electron−hole recombination in TiO_2 materials.

$$2H^+ + 2e^- \rightarrow H_2 \quad E^\circ = -0.41 \tag{1}$$

$$2H_2O + 4h^+ \rightarrow O_2 + 4H^+ \quad E^\circ = +0.82V \tag{2}$$

$$CO_2 + 6H^+ + 6e^- \rightarrow CH_3OH + H_2O \quad E^\circ = -0.38V \tag{3}$$

Special Issue: Alternative Energy Systems

Received: February 27, 2012
Revised: April 30, 2012
Accepted: May 4, 2012
Published: May 5, 2012

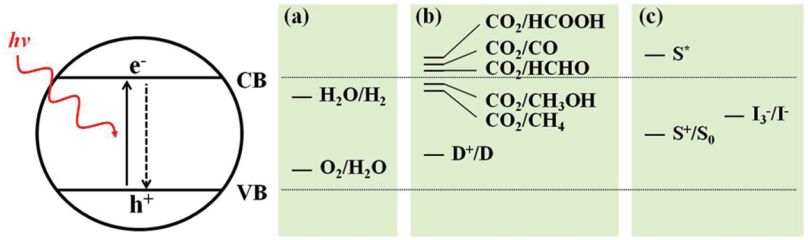

Figure 1. Schematic of TiO_2 photocatalysis and relative positions of redox potentials associated with (a) water splitting, (b) CO_2 reduction, and (c) dye-sensitized solar cells. The redox potentials are not shown on scale. Abbreviations: CB (conduction band), VB (valence band), D (electron donor), S (photosensitizer).

$$CO_2 + 8H^+ + 8e^- \rightarrow CH_4 + 2H_2O \quad E^\circ = -0.24V \tag{4}$$

Mesoscopic thin films of TiO_2 nanoparticles have been used as photoanodes in dye-sensitized solar cells (DSSCs) since the pioneering work by Grätzel and co-workers.[21,22] In a DSSC, effective light harvesting is achieved by using photosensitizers, particularly polypyridyl Ru dye molecules, covalently attached to TiO_2 nanoparticles (Figure 2).[23−26] Upon photoexcitation,

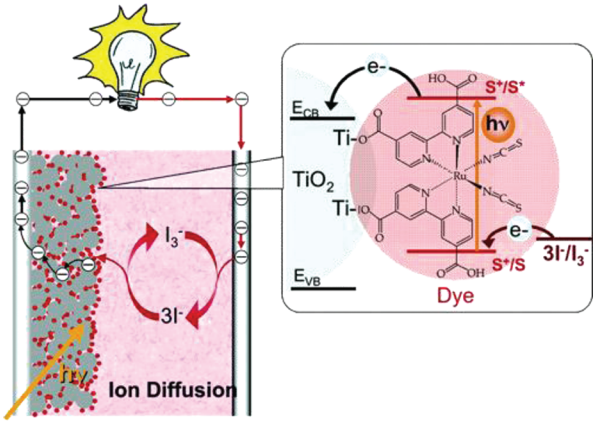

Figure 2. Schematic of a dye-sensitized solar cell. Reprinted with permission from ref 24. Copyright 2005 American Chemical Society.

electrons generated in the dye molecules are rapidly injected into the CB of TiO_2 nanoparticles. The electrons are then collected to generate an electric current in the external circuit. A redox mediator, usually the iodide/triiodide electrolyte (Figure 1c), is employed to shuttle the electrons from a Pt counter electrode to the oxidized dye molecules.[24] Upon recovery of the dye molecules, the net effect of this process is the conversion of a photon into an electron.

The DSSC mechanism has been utilized to design artificial photosynthetic assemblies containing photosensitizers and catalysts linked to TiO_2 surfaces for solar energy applications, including environmental photocatalysis,[27] solar water splitting,[28−30] and solar CO_2 reduction.[31−33] For example, Youngblood and co-workers synthesized an overall water splitting system consisting of a porous nanocrystalline TiO_2 film, heteroleptic ruthenium dye molecules, and hydrated iridium oxide nanoparticles.[30] The ruthenium dye served as a photosensitizer and also a molecular bridge to connect the water-oxidation catalyst (hydrated iridium oxide) to TiO_2 surface. Visible-light water splitting was achieved in the system under a small applied voltage.[30] Armstrong and co-workers modified TiO_2 nanoparticles with ruthenium polypyridyl molecules and enzyme catalysts.[34−36] The functionalized TiO_2 nanoparticles demonstrated excellent activities in photocatalytic H_2 production[34] and CO_2-to-CO coversion[35,36] under visible light irradiation.

3. MIXED-PHASE TiO_2 NANOCOMPOSITES

Coupling two semiconductors can result in spatial separation of photoexcited electrons and holes when the semiconductor band structures are properly aligned.[37−39] A special example of coupled semiconductors is mixed-phase TiO_2 consisting of anatase and rutile, two major polymorphs of TiO_2 materials. Anatase has demonstrated much higher activities than rutile in most studies, partly due to the stronger band bending in anatase relative to rutile.[40] An interesting synergistic effect between anatase and rutile was observed, in which the addition of rutile significantly enhances the activity of anatase.[41−47] Based on the relative CB positions of anatase and rutile, Bickley and co-workers proposed a model involving electron transfer from photoactivated anatase to rutile (Figure 3A).[41] Gray, Rajh,

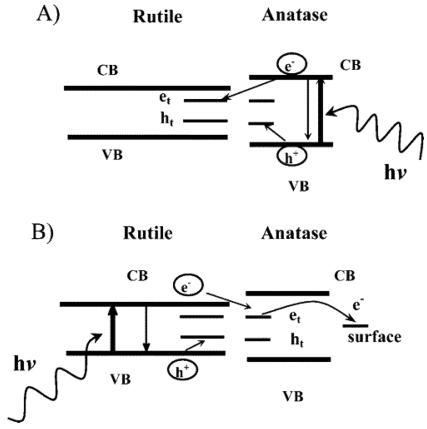

Figure 3. Models for spatial charge separation in mixed-phase TiO_2: (A) Bickley and co-workers' model showing charge separation in anatase and electron trapping in rutile; (B) Gray, Rajh, and co-workers' model of a rutile antenna and subsequent charge separation. Reprinted with permission from ref 44. Copyright 2003 American Chemical Society.

and co-workers studied mixed-phase TiO_2 materials using low-temperature electron paramagnetic resonance (EPR) spectroscopy.[44,45] Trapped electrons in anatase were observed under visible-light irradiation which can only activate the rutile phase in the mixed-phase composite.[44] A mechanism for the synergistic effect was proposed to involve electron transfer from the rutile CB to anatase trapping sites (Figure 3B).[44]

Nair and co-workers proposed an "interfacial model" (Figure 4) to explain the synergistic effect between anatase and rutile.[48]

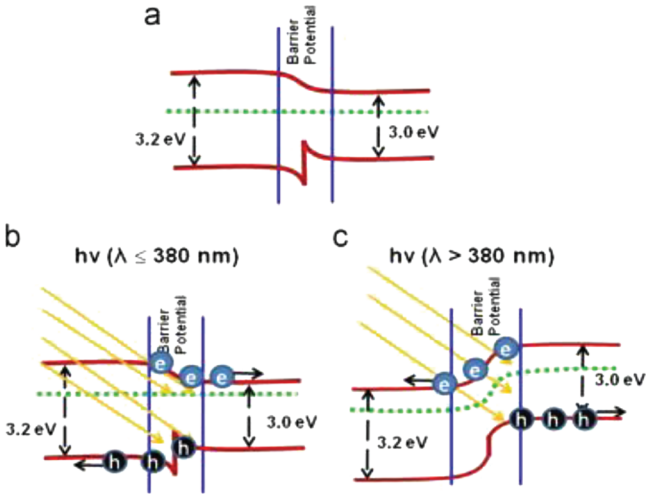

Figure 4. A proposed interfacial band model (a) in the dark, (b) under UV irradiation, and (c) under visible light. The anatase phase (bandgap 3.2 eV) is always shown on the left side and the rutile phase (bandgap 3.0 eV) is shown on the right. Reprinted with permission from ref 48. Copyright 2011 Elsevier B.V.

The "interfacial model" considers band bending at the interfacial region between anatase and rutile. The band structure of the interfacial region in the dark (Figure 4b) is almost the same as under UV irradiation (Figure 4a), although the Fermi level shows an upward shift when both anatase and rutile are activated (Figure 4b).[48] According to the "interfacial model", electron transfer occurs from photoactivated anatase to rutile under UV irradiation since anatase has a more negative CB energy than rutile (Figure 4b).[48] However, under light irradiation with wavelength greater than 380 nm only the rutile phase is activated and the rutile CB shifts upward upon accumulation of photoexcited electrons, making it possible for the photoexcited electrons in rutile to reach the anatase CB (Figure 4c).[48]

Because of the enhanced charge separation, mixed-phase TiO_2 materials demonstrated excellent activity in photocatalytic water splitting[49−51] and CO_2 reduction.[52−54] Interestingly, recent studies indicate that mixed-phase TiO_2 materials are better than pure anatase or rutile in DSSCs,[55−59] in which photoexcited electrons are generated in the dye molecules instead of TiO_2 nanoparticles. Anatase TiO_2 is often used to prepare photoanodes in DSSCs partly because of the excellent electron mobility in anatase CB. The fabrication of DSSC photoanodes usually involves treatment with a dilute solution of $TiCl_4$ prior to dye sensitization,[60] which significantly improves the photocurrent and efficiency of anatase TiO_2 thin films. Different explanations have been proposed for the beneficial effect of the $TiCl_4$ treatment, including the formation of a new rutile layer upon the $TiCl_4$ treatment.[61] Li and co-workers observed the synergistic effect between anatase and rutile when mixed-phase TiO_2 composites were used as photoanodes in DSSCs.[62] The mixed-phase TiO_2 composites were prepared by adding different amounts of rutile nanorods to anatase nanoparticles. The addition of 10−15% rutile significantly enhanced light harvesting and the overall photovoltaic efficiency of anatase TiO_2 in DSSCs.[62] Using time-resolved terahertz spectroscopy, the researchers clearly demonstrated that interfacial electron transfer from dye-sensitized rutile to anatase contributed to the enhanced photovoltaic performance of mixed-phase TiO_2 photoanodes.[62] A mechanism similar to the "interfacial model" was suggested, in which the accumulation of photoexcited electrons in rutile led to an upward shift of the rutile CB (Figure 4c) and subsequently enabled interfacial electron transfer from rutile to anatase.[62]

In mixed-phase TiO_2, the interfacial nanostructures strongly influence electron transfer between the individual components and photocatalytic efficiency.[63−67] Zhang and co-workers investigated mixed-phase TiO_2 in photocatalytic H_2 evolution from methanol/water solutions.[46] Their studies using UV Raman spectroscopy and high-resolution transmission electron microscopy demonstrated that the phase junction between anatase and rutile significantly enhanced the photocatalytic activity of the mixed-phase material.[46] Furthermore, Gray, Rajh, and co-workers identified[44] and explained[68] the existence of interfacial tetrahedral Ti sites in mixed-phase TiO_2, which are highly active sites in photocatalysis.

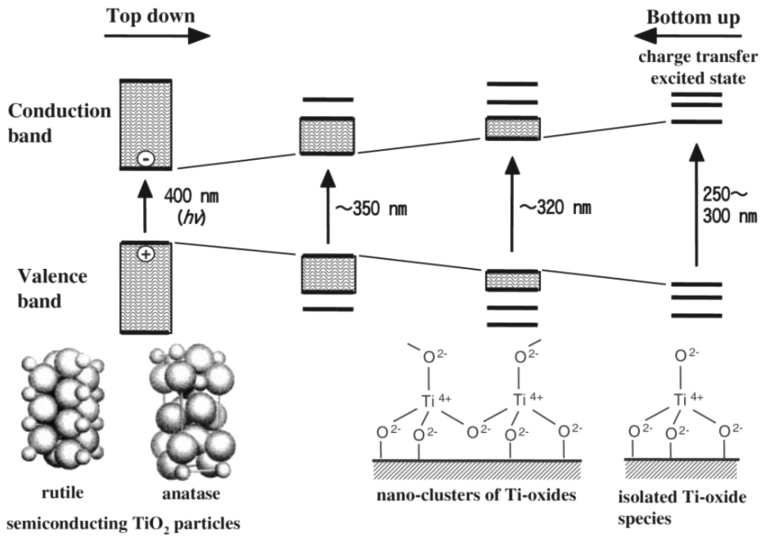

Figure 5. Size quantization effect: structures and electronic states of bulk TiO_2 particles, molecular-scale titanium oxide clusters, and isolated single-site titanium oxide species. Reprinted with permission from ref 70. Copyright 2004 the Chemical Society of Japan.

4. HIGHLY DISPERSED TITANIUM OXIDE PHOTOCATALYSTS

Anpo and co-workers observed that photocatalytic activities of TiO_2 particles markedly increased as the particle sizes became smaller than 10 nm and that the observed size quantization effect did not arise from changes in specific surface areas.[69] Instead, the surface-to-bulk ratio increased as the particle size decreased, resulting in shorter diffusion paths for the photogenerated electrons and holes to reach the surfaces of smaller TiO_2 particles where photocatalytic reactions occur.[70] Therefore, enhanced charge separation and improved photocatalysis could be achieved by using TiO_2 nanoparticles, particularly in the presence of surface adsorbed species which function as electron or hole scavengers. Koci and co-workers investigated the activities of anatase nanoparticles with crystal sizes ranging from 4.5 to 29 nm in photocatalytic CO_2 reduction.[71] The researchers observed that the 14-nm anatase gave the highest yields of both methane and methanol as the CO_2-reduction products.[71] The observed size effect was attributed to a combination of factors including specific surface area, charge-carrier dynamics, and light absorption capacity.[71]

An undesired consequence of size quantization is the shift of TiO_2 absorption edges toward the UV region (Figure 5).[70] For instance, the threshold absorption wavelength of rutile TiO_2 particles shifted from 410.4 to 398.0 nm when the particle size changed from 200 to 5.5 nm, accounting for an increase of 0.0934 eV in the TiO_2 bandgap.[70] In addition, very small TiO_2 nanoparticles, especially those synthesized by solution-phase methods, are unstable in the absence of surface functional groups. The nanoparticles tend to aggregate upon thermal treatment that is necessary for achieving good crystallinity and high photocatalytic activity. This problem can be solved by synthesizing TiO_2 nanoparticles or nanoclusters in confined environment such as zeolite cavities. White and Dutta synthesized anatase TiO_2 nanoclusters encapsulated in zeolite Y by ion-exchanging a molecular titanium precursor, ammonium titanyl oxalate, into the zeolite pores.[72] Clusters of CdS as a narrow-bandgap photosensitizer and metallic Pt as a catalyst for hydrogen production were also synthesized in the zeolite pores following the same approach.[72] Photocatalytic hydrogen evolution was observed using the sensitized TiO_2 nanoclusters in the presence of the S^{2-}/SO_3^{2-} sacrificial electron donor system.[72]

Using the same ion-exchange synthesis, Anpo and co-workers prepared highly dispersed titanium oxide clusters in zeolite Y, which exhibited high reactivity in photocatalytic CO_2 reduction using H_2O as the reducing agent under UV irradiation.[73−75] Spatially separated titanium oxide species were further prepared as single-site photocatalysts by incorporating titanium atoms in the framework of mesoporous zeolites.[76−83] Frei and co-workers observed CO as the sole product of CO_2 reduction by H_2O on framework titanium centers in Ti-MCM-41 silicate sieves under UV light.[78] In the studies by Anpo and co-workers, the selective formation of CH_3OH and CH_4 via CO_2 reduction was observed on single-site titanium oxides under UV irradiation.[84]

The titanium coordination of highly dispersed titanium oxides has profound influence on the reactivity and selectivity in photocatalytic CO_2 reduction (Figure 6).[85] For example, the quantum yield for the formation of CH_3OH and CH_4 in photocatalytic CO_2 reduction on Ti-containing mesoporous silica was estimated to be 0.28% in comparison with 0.005% on bulk TiO_2 particles.[70] It was revealed that highly dispersed titanium oxide species in tetrahedral coordination were responsible for the high selectivity toward the formation of CH_3OH due to the charge-transfer excited state, $(Ti^{3+}\text{-}O^-)^*$, of the titanium oxides in zeolites.[73,74] On the other hand, aggregated titanium oxides in octahedral coordination were found to be associated with CH_4 production, similar to what was observed in CO_2 reduction on bulk TiO_2 photocatalysts.[73,74] It was determined that the charge-transfer excited state of highly dispersed titanium oxides has a much longer lifetime (microseconds) than that of bulk TiO_2 materials (nanoseconds).[77] Therefore, the formation of long-lived, localized charge-transfer excited states contributed to the improved CO_2-reduction activity of highly dispersed titanium oxide photocatalysts.

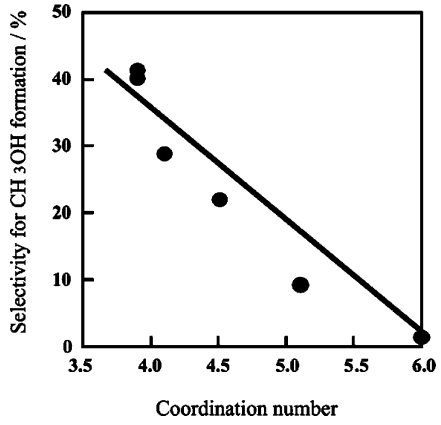

Figure 6. Correlation between the selectivity of CH_3OH formation in photocatalytic reduction of CO_2 with H_2O and the coordination number of titanium oxide species incorporated within zeolites. The coordination number was obtained from X-ray absorption fine structure analyses. Reprinted with permission from ref 85. Copyright 2003 Elsevier Science (USA).

Tetrahedrally coordinated titanium oxides have been utilized to form all-inorganic metal-to-metal charge transfer (MMCT) complexes anchored in mesoporous silica which can be activated by visible light.[86,87] The MMCT complexes are oxo-bridged heteronuclear species TiOM (M = Mn, Sn, Cu, Co, Ce and Cr) with appropriately chosen redox potentials.[88,89] Upon visible-light photoexcitation, electron transfer from M (donor) to Ti (acceptor) results in the formation of transient species including Ti^{3+}. In the recent work by Frei and co-workers, it was shown that the MMCT excited state of a TiOMn chromophore has an unusually long lifetime in the microsecond scale due to strong polarization of the silica environment upon photoexcited electron transfer from Mn to Ti.[88] The long lifetime of the MMCT excited state suggests that the oxo-bridged heteronuclear units are promising charge-transfer chromophores for driving multielectron catalysts in artificial photosynthetic systems.[88] In fact, a TiOCr chromophore has been coupled with iridium oxide nanoclusters for use in visible-light water oxidation.[90]

Titanium oxides confined in microporous and mesoporous zeolites were also evaluated in photovoltaic applications. Atienzar and co-workers prepared titanium-containing zeolites which demonstrated photovoltaic activities.[91] The photoresponse of dye-sensitized zeolites was independent of the zeolite pore dimensions or particle sizes, but increased with titanium content.[91] The researchers also investigated Ti-MCM-

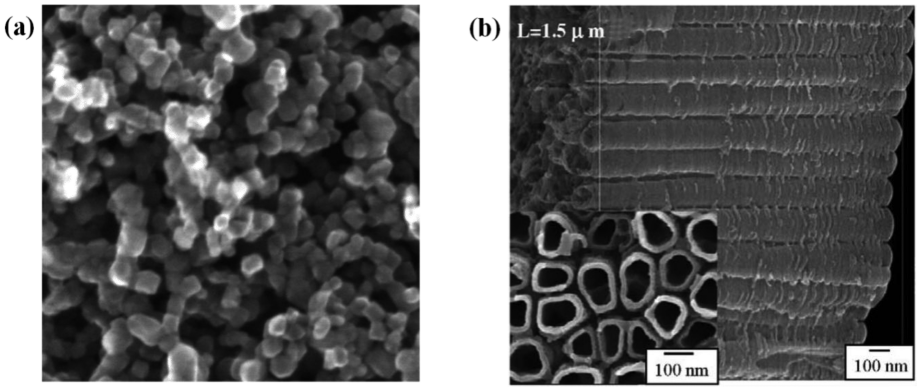

Figure 7. (a) Scanning electron micrograph of mesoporous TiO_2 nanoparticles deposited on a conducting glass as the photoanode of a DSSC. The average particle size is 20 nm. Reprinted with permission from ref 24. Copyright 2005 American Chemical Society. (b) Scanning electron micrograph of highly ordered TiO_2 nanotube arrays prepared by anodization. Reprinted with permission from ref 103. Copyright 2006 Elsevier B. V.

41, which contains isolated titanium atoms in the framework of mesoporous silica, as the photoanode of a DSSC.[92] The measured photocurrent per titanium atom for the Ti-MCM-41 was very similar to that of a commercially available TiO_2 material having an average particle size of 25 nm.[92]

5. SOLAR ENERGY CONVERSION USING TiO_2 NANOTUBES

As discussed earlier, enhanced photocatalysis can be achieved by controlling particle sizes and nanostructures of TiO_2 materials.[93] The photocatalytic and photovoltaic properties of TiO_2 materials can also be improved by adopting new morphologies, such as nanotubes which have attracted enormous attention.[94−97] In TiO_2 nanotubes, photoexcited electrons and holes could move along the nanotubes, leading to increased delocalization and long diffusion length of charge carriers (>200 nm).[98−100] As a result, charge recombination is retarded by the tubular morphology of TiO_2 nanotubes. This feature is particularly advantageous for photovoltaic and photocatalytic applications.[101−106] In a conventional DSSC, the photoanode consists of interconnected TiO_2 nanoparticles which are deposited on a conducting glass, forming a mesoporous thin film (Figure 7a).[24] Electrons generated in the dye molecules are injected into the conduction band of TiO_2 nanoparticles. The electrons then diffuse through the three-dimensional network of TiO_2 nanoparticles to reach the conducting glass before being collected as an electric current in the external circuit. The DSSC efficiency is strongly influenced by interfacial nanostructures and connection between individual TiO_2 nanoparticles. Furthermore, the electrons may be intercepted by triiodide in the electrolyte solution during the diffusion process across the TiO_2 network. Loss of photogenerated electrons during the diffusion process could potentially be prevented by using vertically aligned TiO_2 nanotube arrays to collect the electron (Figure 7b).[103] In DSSCs using TiO_2 nanotubes instead of TiO_2 nanoparticles, it is expected that photogenerated electrons could travel along the nanotubes to reach the external circuit. The much higher electron diffusion length in nanotubes than in nanoparticles suggests that the tubular morphology could contribute to improved photovoltaic efficiency. Figure 8 shows the schematic diagram of a DSSC consisting of highly ordered TiO_2 nanotubes.[103] The self-standing nanotube array was fabricated by anodic oxidation of a titanium foil.[103] In the configuration shown in Figure 8, the titanium foil supporting the nanotubes

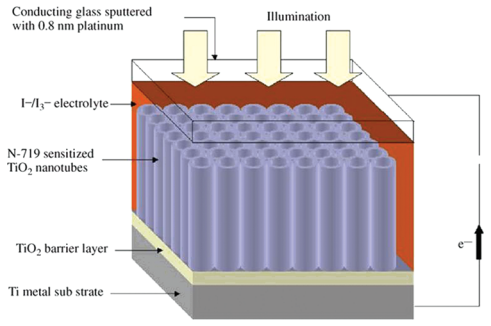

Figure 8. Schematic diagram of a DSSC using dye-sensitized TiO_2 nanotubes. Reprinted with permission from ref 103. Copyright 2006 Elsevier B. V.

serves as the conducting substrate to replace a conducting glass which is widely used in conventional DSSCs. As a result, the DSSC is illuminated through the more transparent Pt counter electrode.

Current solar cell conversion efficiencies using TiO_2 nanotubes are in the range of 4−5%,[101] much lower than the record of 11.2% using TiO_2 nanoparticles[107] when polypyridyl ruthenium dyes are used as the photosensitizer. The photovoltaic performance of TiO_2 nanotubes could be further improved by optimizing parameters, including nanotube geometry and microstructures which strongly influence electron transport, recombination kinetics, and solar energy conversion efficiencies.[101] Zhu and co-workers investigated the effect of thermal treatment on the photovoltaic performance of TiO_2 nanotubes.[108] Thermal treatment in the range between 200 and 600 °C significantly improved crystallinity while inducing phase transformation of as-deposited TiO_2 nanotube arrays.[108] Annealing at high temperatures also led to partial degradation of the nanotube walls. The researchers then demonstrated that nanotube films annealed at 400 °C exhibited the highest morphological order, fastest electron transport, slowest recombination kinetics, and subsequently highest solar energy conversion efficiency.[108]

Following the DSSC configuration shown in Figure 8, highly ordered TiO_2 nanotube arrays have been investigated in photoelectrochemical water splitting,[103] in which water oxidation occurs on the photoanode in the presence of overpotentials. For example, Park and co-workers prepared TiO_2 nanotube arrays for use in solar water splitting.[109] The water-splitting photocurrent produced by the TiO_2 nanotube

arrays was more than 10 times higher than that of TiO_2 nanoparticles.[109] It was suggested that the improved performance of the TiO_2 nanotube arrays originated from better light harvesting and charge separation of the TiO_2 nanotubes in comparison with TiO_2 nanoparticles.[109]

Additional components could be incorporated within the TiO_2 nanotubes, forming nanocomposites that further improve light harvesting and charge separation. For instance, CdS nanoparticles as photosensitizers have been attached to TiO_2 nanotubes for use in water splitting under visible light irradiation.[110,111] Feng and co-workers deposited ultrafine Pt nanoparticles within TiO_2 nanotubes, which demonstrated excellent activity in photocatalytic conversion of CO_2 and H_2O into CH_4.[112] The TiO_2 nanotube surface allowed homogeneous distribution of Pt nanoparticles as the electron sinks and active reduction sites, enabling efficient charge separation.[112]

6. CONCLUSIONS

Semiconducting TiO_2 materials have been extensively investigated in photocatalytic and photovoltaic applications. Solar energy conversion efficiencies of TiO_2 materials largely depend on the extent of charge separation between photoexcited electrons and holes. This article discusses three effective strategies that have resulted in hindered charge recombination in TiO_2 materials. In mixed-phase TiO_2, photogenerated electrons and holes get trapped in different phases (anatase or rutile), leading to spatial charge separation. The charge-transfer excited state of highly dispersed titanium oxides has a much longer lifetime than that of bulk TiO_2 materials. As a result, enhanced photoactivity and selectivity in CO_2 reduction was achieved using highly dispersed titanium oxides with relatively low titanium coordination numbers. Nanotubular TiO_2 materials show great promise in both photocatalytic and photovoltaic applications because of the long diffusion length of charge carriers along the nanotube axis.

It should be pointed out that many other factors beyond charge separation could significantly influence the overall solar energy conversion efficiencies in photocatalytic and photovoltaic processes. For instance, the adsorption and reaction of substrate molecules on TiO_2 surfaces are among the essential steps of heterogeneous photocatalysis,[1] while the adsorption of dye molecules[113] and charge transfer dynamics at the dye–TiO_2 interfaces are more important in DSSCs.[23] Because the operational principles of photocatalysis and photovoltaics are different, a highly active TiO_2 photocatalyst does not necessarily perform well in a DSSC and vice versa.

This article is based on selected examples from the literature demonstrating how improved charge separation is achieved through the three approaches. It can be seen from the examples that significant advances have been made in recent years in the field of solar energy conversion using TiO_2 materials. Although research on alternative photocatalysts to TiO_2[114,115] has been equally successful, TiO_2 remains the most promising material for photocatalytic and photovoltaic applications.

AUTHOR INFORMATION

Corresponding Author

*E-mail: gonghu.li@unh.edu.

Notes

The authors declare no competing financial interest.

ACKNOWLEDGMENTS

We are thankful for support from the U.S. National Science Foundation through the Nanoscale Science & Engineering Center for High-rate Nanomanufacturing (NSF EEC 0832785).

REFERENCES

(1) Linsebigler, A. L.; Lu, G. Q.; Yates, J. T. Photocatalysis on TiO_2 Surfaces - Principles, Mechanisms, and Selected Results. *Chem. Rev.* **1995**, *95*, 735–758.
(2) Kamat, P. V. Photochemistry on nonreactive and reactive (semiconductor) surfaces. *Chem. Rev.* **1993**, *93*, 267–300.
(3) Henderson, M. A. A surface science perspective on TiO_2 photocatalysis. *Surf. Sci. Rep.* **2011**, *66*, 185–297.
(4) Carp, O.; Huisman, C. L.; Reller, A. Photoinduced reactivity of titanium dioxide. *Prog. Solid State Chem.* **2004**, *32*, 33–177.
(5) Kabra, K.; Chaudhary, R.; Sawhney, R. L. Treatment of Hazardous Organic and Inorganic Compounds through Aqueous-Phase Photocatalysis: A Review. *Ind. Eng. Chem. Res.* **2004**, *43*, 7683–7696.
(6) Diebold, U. The surface science of titanium dioxide. *Surf. Sci. Rep.* **2003**, *48*, 53–229.
(7) Hoffmann, M. R.; Martin, S. T.; Choi, W. Y.; Bahnemann, D. W. Environmental Applications of Semiconductor Photocatalysis. *Chem. Rev.* **1995**, *95*, 69–96.
(8) Fox, M. A.; Dulay, M. T. Heterogeneous Photocatalysis. *Chem. Rev.* **1993**, *93*, 341–357.
(9) Kumar, S. G.; Devi, L. G. Review on modified TiO_2 photocatalysis under UV/Visible light: Selected results and related mechanisms on interfacial charge carrier transfer dynamics. *J. Phys. Chem. A* **2011**, *115*, 13211–13241.
(10) Kamat, P. V. Meeting the Clean Energy Demand: Nanostructure Architectures for Solar Energy Conversion. *J. Phys. Chem. C* **2007**, *111*, 2834–2860.
(11) Kitano, M.; Matsuoka, M.; Ueshima, M.; Anpo, M. Recent developments in titanium oxide-based photocatalysts. *Appl. Catal., A* **2007**, *325*, 1–14.
(12) Fujishima, A.; Honda, K. Electrochemical Photolysis of Water at a Semiconductor Electrode. *Nature* **1972**, *238*, 37–38.
(13) Inoue, T.; Fujishima, A.; Konishi, S.; Honda, K. Photoelectrocatalytic reduction of carbon dioxide in aqueous suspensions of semiconductor powders. *Nature* **1979**, *277*, 637–638.
(14) Chen, X.; Shen, S.; Guo, L.; Mao, S. S. Semiconductor-based Photocatalytic Hydrogen Generation. *Chem. Rev.* **2010**, *110*, 6503–6570.
(15) Hoffmann, M. R.; Moss, J. A.; Baum, M. M. Artificial photosynthesis: Semiconductor photocatalytic fixation of CO_2 to afford higher organic compounds. *Dalton Trans.* **2011**, *40*, 5151–5158.
(16) Joshi, U. A.; Palasyuk, A.; Arney, D.; Maggard, P. A. Semiconducting Oxides to Facilitate the Conversion of Solar Energy to Chemical Fuels. *J. Phys. Chem. Lett.* **2010**, *1*, 2719–2726.
(17) Indrakanti, V. P.; Kubicki, J. D.; Schobert, H. H. Photoinduced activation of CO_2 on Ti-based heterogeneous catalysts: Current state, chemical physics-based insights and outlook. *Energy Environ. Sci.* **2009**, *2*, 745–758.
(18) Usubharatana, P.; McMartin, D.; Veawab, A.; Tontiwachwuthikul, P. Photocatalytic Process for CO_2 Emission Reduction from Industrial Flue Gas Streams. *Ind. Eng. Chem. Res.* **2006**, *45*, 2558–2568.
(19) Fujita, E.; Muckerman, J. T. Catalytic Reactions Using Transition-Metal-Complexes Toward Solar Fuel Production. *Bull. Jpn. Soc. Coord. Chem.* **2008**, *51*, 41–54.
(20) Fujita, E. Photochemical carbon dioxide reduction with metal complexes. *Coord. Chem. Rev.* **1999**, *185–186*, 373–384.
(21) O'Regan, B.; Grätzel, M. A low-cost, high-efficiency solar cell based on dye-sensitized colloidal TiO_2 films. *Nature* **1991**, *353*, 737–740.

(22) Yella, A.; Lee, H.-W.; Tsao, H. N.; Yi, C.; Chandiran, A. K.; Nazeeruddin, M. K.; Diau, E. W.-G.; Yeh, C.-Y.; Zakeeruddin, S. M.; Graetzel, M. Porphyrin-Sensitized Solar Cells with Cobalt (II/III)-Based Redox Electrolyte Exceed 12% Efficiency. *Science* **2011**, *334*, 629−634.
(23) Grätzel, M. Photoelectrochemical cells. *Nature* **2001**, *414*, 338−344.
(24) Grätzel, M. Solar Energy Conversion by Dye-Sensitized Photovoltaic Cells. *Inorg. Chem.* **2005**, *44*, 6841−6851.
(25) Meyer, G. J. Molecular Approaches to Solar Energy Conversion with Coordination Compounds Anchored to Semiconductor Surfaces. *Inorg. Chem.* **2005**, *44*, 6852−6864.
(26) Hagfeldt, A.; Boschloo, G.; Sun, L.; Kloo, L.; Pettersson, H. Dye-Sensitized Solar Cells. *Chem. Rev.* **2010**, *110*, 6595−6663.
(27) Chowdhury, P.; Moreira, J.; Gomaa, H.; Ray, A. K. Visible-Solar-Light-Driven Photocatalytic Degradation of Phenol with Dye-Sensitized TiO_2: Parametric and Kinetic Study. *Ind. Eng. Chem. Res.* **2012**, *51*, 4523−4532.
(28) Song, W.; Chen, Z.; Brennaman, M. K.; Concepcion, J. J.; Patrocinio, A. O. T.; Iha, N. Y. M.; Meyer, T. J. Making solar fuels by artificial photosynthesis. *Pure Appl. Chem.* **2011**, *83*, 749−768.
(29) Li, G.; Sproviero, E. M.; McNamara, W. R.; Snoeberger, R. C. I.; Crabtree, R. H.; Brudvig, G. W.; Batista, V. S. Reversible Visible-Light Photooxidation of an Oxomanganese Water-Oxidation Catalyst Covalently Anchored to TiO_2 Nanoparticles. *J. Phys. Chem. B* **2010**, *114*, 14214−14222.
(30) Youngblood, W. J.; Lee, S.-H. A.; Kobayashi, Y.; Hernandez-Pagan, E. A.; Hoertz, P. G.; Moore, T. A.; Moore, A. L.; Gust, D.; Mallouk, T. E. Photoassisted Overall Water Splitting in a Visible Light-Absorbing Dye-Sensitized Photoelectrochemical Cell. *J. Am. Chem. Soc.* **2009**, *131*, 926−927.
(31) Nguyen, T.-V.; Wu, J. C. S.; Chiou, C.-H. Photoreduction of CO_2 over ruthenium dye-sensitized TiO_2-based catalysts under concentrated natural sunlight. *Catal. Commun.* **2008**, *9*, 2073−2076.
(32) Ozcan, O.; Yukruk, F.; Akkaya, E. U.; Uner, D. Dye sensitized CO_2 reduction over pure and platinized TiO_2. *Top. Catal* **2007**, *44*, 523−528.
(33) Ozcan, O.; Yukruk, F.; Akkaya, E. U.; Uner, D. Dye sensitized artificial photosynthesis in the gas phase over thin and thick TiO_2 films under UV and visible light irradiation. *Appl. Catal., B* **2007**, *71*, 291−297.
(34) Reisner, E.; Powell, D. J.; Cavazza, C.; Fontecilla-Camps, J. C.; Armstrong, F. A. Visible Light-Driven H_2 Production by Hydrogenases Attached to Dye-Sensitized TiO_2 Nanoparticles. *J. Am. Chem. Soc.* **2009**, *131*, 18457−18466.
(35) Woolerton, T. W.; Sheard, S.; Reisner, E.; Pierce, E.; Ragsdale, S. W.; Armstrong, F. A. Efficient and Clean Photoreduction of CO_2 to CO by Enzyme-Modified TiO_2 Nanoparticles Using Visible Light. *J. Am. Chem. Soc.* **2010**, *132*, 2132−2133.
(36) Woolerton, T. W.; Sheard, S.; Pierce, E.; Ragsdale, S. W.; Armstrong, F. A. CO_2 photoreduction at enzyme-modified metal oxide nanoparticles. *Energy Environ. Sci.* **2011**, *4*, 2393−2399.
(37) Serpone, N.; Maruthamuthu, P.; Pichat, P.; Pelizzetti, E.; Hidaka, H. Exploiting the Interparticle Electron-Transfer Process in the Photocatalyzed Oxidation of Phenol, 2-Chlorophenol and Pentachlorophenol - Chemical Evidence for Electron and Hole Transfer between Coupled Semiconductors. *J. Photochem. Photobiol., A* **1995**, *85*, 247−255.
(38) Rajeshwar, K.; de Tacconi, N. R.; Chenthamarakshan, C. R. Semiconductor-based composite materials: Preparation, properties, and performance. *Chem. Mater.* **2001**, *13*, 2765−2782.
(39) Nevins, J. S.; Coughlin, K. M.; Watson, D. F. Attachment of CdSe Nanoparticles to TiO_2 via Aqueous Linker-Assisted Assembly: Influence of Molecular Linkers on Electronic Properties and Interfacial Electron Transfer. *ACS Appl. Mater. Interfaces* **2011**, *3*, 4242−4253.
(40) Li, G.; Chen, L.; Graham, M. E.; Gray, K. A. A Comparison of Mixed Phase Titania Photocatalysts Prepared by Physical and Chemical Methods: The Importance of the Solid-solid Interface. *J. Mol. Catal. A* **2007**, *275*, 30−35.
(41) Bickley, R. I.; Gonzalezcarreno, T.; Lees, J. S.; Palmisano, L.; Tilley, R. J. D. A Structural Investigation of Titanium-Dioxide Photocatalysts. *J. Solid State Chem.* **1991**, *92*, 178−190.
(42) Ohno, T.; Sarukawa, K.; Tokieda, K.; Matsumura, M. Morphology of a TiO_2 photocatalyst (Degussa, P-25) consisting of anatase and rutile crystalline phases. *J. Catal.* **2001**, *203*, 82−86.
(43) Ohno, T.; Tokieda, K.; Higashida, S.; Matsumura, M. Synergism between rutile and anatase TiO_2 particles in photocatalytic oxidation of naphthalene. *Appl. Catal., A* **2003**, *244*, 383−391.
(44) Hurum, D. C.; Agrios, A. G.; Gray, K. A.; Rajh, T.; Thurnauer, M. C. Explaining the enhanced photocatalytic activity of Degussa P25 mixed-phase TiO_2 using EPR. *J. Phys. Chem. B* **2003**, *107*, 4545−4549.
(45) Hurum, D. C.; Agrios, A. G.; Crist, S. E.; Gray, K. A.; Rajh, T.; Thurnauer, M. C. Probing reaction mechanisms in mixed phase TiO_2 by EPR. *J. Electron Spectrosc. Relat. Phenom.* **2006**, *150*, 155−163.
(46) Zhang, J.; Xu, Q.; Feng, Z.; Li, M.; Li, C. Importance of the relationship between surface phases and photocatalytic activity of TiO_2. *Angew. Chem., Int. Ed.* **2008**, *47*, 1766−1769.
(47) Su, R.; Bechstein, R.; Sø, L.; Vang, R. T.; Sillassen, M.; Esbjörnsson, B.; Palmqvist, A.; Besenbacher, F. How the Anatase-to-Rutile Ratio Influences the Photoreactivity of TiO_2. *J. Phys. Chem. C* **2011**, *115*, 24287−24292.
(48) Nair, R. G.; Paul, S.; Samdarshi, S. K. High UV/visible light activity of mixed phase titania: A generic mechanism. *Sol. Energy Mater. Sol. Cells* **2011**, *95*, 1901−1907.
(49) Liu, M.; de, L. S. N.; Park, H. Water photolysis with a cross-linked titanium dioxide nanowire anode. *Chem. Sci.* **2011**, *2*, 80−87.
(50) Luo, H.; Takata, T.; Lee, Y.; Zhao, J.; Domen, K.; Yan, Y. Photocatalytic Activity Enhancing for Titanium Dioxide by Co-doping with Bromine and Chlorine. *Chem. Mater.* **2004**, *16*, 846−849.
(51) Lin, C.-J.; Tu, W.-K.; Kuo, C.-K.; Chien, S.-H. Single-step fabrication of phase-controllable nanocrystalline TiO_2 films for enhanced photoelectrochemical water splitting and dye-sensitized solar cells. *J. Power Sources* **2011**, *196*, 4865−4869.
(52) DeSario, P. A.; Chen, L.; Graham, M. E.; Gray, K. A. Effect of oxygen deficiency on the photoresponse and reactivity of mixed phase titania thin films. *J. Vac. Sci. Technol., A* **2011**, *29*, 031508/1−031508/7.
(53) Chen, L.; Graham, M. E.; Li, G.; Gentner, D. R.; Dimitrijevic, N.; Gray, K. A. Photoreduction of CO_2 by TiO_2 nanocomposites synthesized through reactive direct current magnetron sputter deposition. *Thin Solid Films* **2009**, *517*, 5641−5645.
(54) Li, G.; Ciston, S.; Saponjic, Z.; Chen, L.; Dimitrijevic, N.; Rajh, T.; Gray, K. A. Synthesizing Mixed Phase TiO_2 Nanocomposites Using a Hydrothermal Method for Photooxidation and Photoreduction Applications. *J. Catal.* **2008**, *253*, 105−110.
(55) Park, J. T.; Koh, J. H.; Seo, J. A.; Kim, J. H. Formation of mesoporous TiO_2 with large surface areas, interconnectivity and hierarchical pores for dye-sensitized solar cells. *J. Mater. Chem.* **2011**, *21*, 17872−17880.
(56) Kim, B.-M.; Rho, S.-G.; Kang, C.-H. Effects of TiO_2 structures in dye-sensitized solar cell. *J. Nanosci. Nanotechnol.* **2011**, *11*, 1515−1517.
(57) Zhu, Q.; Qian, J.; Pan, H.; Tu, L.; Zhou, X. Synergistic manipulation of micro-nanostructures and composition: anatase/rutile mixed-phase TiO_2 hollow micro-nanospheres with hierarchical mesopores for photovoltaic and photocatalytic applications. *Nanotechnology* **2011**, *22*, 395703/1−395703/9 S395703/1-S395703/6.
(58) Peng, W.; Yanagida, M.; Han, L. Rutile-anatase TiO_2 photoanodes for dye-sensitized solar cells. *J. Nonlinear Opt. Phys. Mater.* **2010**, *19*, 673−679.
(59) Kang, S. H.; Lim, J.-W.; Kim, H. S.; Kim, J.-Y.; Chung, Y.-H.; Sung, Y.-E. Photo and Electrochemical Characteristics Dependent on the Phase Ratio of Nanocolumnar Structured TiO_2 Films by RF Magnetron Sputtering Technique. *Chem. Mater.* **2009**, *21*, 2777−2788.
(60) Ito, S.; Murakami, T. N.; Comte, P.; Liska, P.; Grätzel, C.; Nazeeruddin, M. K.; Grätzel, M. Fabrication of thin film dye sensitized solar cells with solar to electric power conversion efficiency over 10%. *Thin Solid Films* **2008**, *516*, 4613−4619.

(61) Kambe, S.; Nakade, S.; Wada, Y.; Kitamura, T.; Yanagida, S. Effects of crystal structure, size, shape and surface structural differences on photo-induced electron transport in TiO_2 mesoporous electrodes. *J. Mater. Chem.* **2002**, *12*, 723−728.
(62) Li, G.; Richter, C.; Milot, R. L.; Cai, L.; Schmuttenmaer, C. A.; Crabtree, R. H.; Brudvig, G. W.; Batista, V. S. Synergistic effect between anatase and rutile TiO_2 nanoparticles in dye-sensitized solar cells. *Dalton Trans.* **2009**, 10078−10085.
(63) Zhang, X.; Lin, Y.; He, D.; Zhang, J.; Fan, Z.; Xie, T. Interface junction at anatase/rutile in mixed-phase TiO_2. Formation and photogenerated charge carriers properties. *Chem. Phys. Lett.* **2011**, *504*, 71−75.
(64) Xu, Q.; Ma, Y.; Zhang, J.; Wang, X.; Feng, Z.; Li, C. Enhancing hydrogen production activity and suppressing CO formation from photocatalytic biomass reforming on Pt/TiO_2 by optimizing anatase-rutile phase structure. *J. Catal.* **2011**, *278*, 329−335.
(65) Li, G.-L.; Li, W.-X.; Li, C. Model relation between the energy-band edge and the Fermi level of the nondegenerate semiconductor TiO_2: Application to electrochemistry. *Phys. Rev. B* **2010**, *82*, 235109/1−235109/8.
(66) Li, G.; Gray, K. A. The Solid-Solid Interface: Explaining the High and Unique Photocatalytic Reactivity of TiO_2-Based Nanocomposite Materials. *Chem. Phys.* **2007**, *339*, 173−187.
(67) Deskins, N. A.; Kerisit, S.; Rosso, K. M.; Dupuis, M. Molecular Dynamics Characterization of Rutile-Anatase Interfaces. *J. Phys. Chem. C* **2007**, *111*, 9290−9298.
(68) Li, G.; Dimitrijevic, N.; Chen, L.; Nichols, J.; Rajh, T.; Gray, K. A. The Important Role of Tetrahedral Ti^{4+} Sites in the Phase Transformation and Photocatalyt Activity of TiO_2 Nanocomposites. *J. Am. Chem. Soc.* **2008**, *130*, 5402−5403.
(69) Anpo, M.; Shima, T.; Kodama, S.; Kubokawa, Y. Photocatalytic hydrogenation of propyne with water on small-particle titania: Size quantization effects and reaction intermediates. *J. Phys. Chem.* **1987**, *91*, 4305−10.
(70) Anpo, M. Preparation, characterization, and reactivities of highly functional titanium oxide-based photocatalysts able to operate under UV-visible light irradiation: Approaches in realizing high efficiency in the use of visible light. *Bull. Chem. Soc. Jpn.* **2004**, *77*, 1427−1442.
(71) Koci, K.; Obalova, L.; Matejova, L.; Placha, D.; Lacny, Z.; Jirkovsky, J.; Solcova, O. Effect of TiO_2 particle size on the photocatalytic reduction of CO_2. *Appl. Catal., B* **2009**, *89*, 494−502.
(72) White, J. C.; Dutta, P. K. Assembly of Nanoparticles in Zeolite Y for the Photocatalytic Generation of Hydrogen from Water. *J. Phys. Chem. C* **2011**, *115*, 2938−2947.
(73) Yamashita, H.; Fujii, Y.; Ichihashi, Y.; Zhang, S. G.; Ikeue, K.; Park, D. R.; Koyano, K.; Tatsumi, T.; Anpo, M. Selective formation of CH_3OH in the photocatalytic reduction of CO_2 with H_2O on titanium oxides highly dispersed within zeolites and mesoporous molecular sieves. *Catal. Today* **1998**, *45*, 221−227.
(74) Anpo, M.; Yamashita, H.; Ichihashi, Y.; Fujii, Y.; Honda, M. Photocatalytic Reduction of CO_2 with H_2O on Titanium Oxides Anchored within Micropores of Zeolites: Effects of the Structure of the Active Sites and the Addition of Pt. *J. Phys. Chem. B* **1997**, *101*, 2632−2636.
(75) Anpo, M.; Yamashita, H.; Ichihashi, Y.; Ehara, S. Photocatalytic reduction of CO_2 with H_2O on various titanium oxide catalysts. *J. Electroanal. Chem.* **1995**, *396*, 21−26.
(76) Anpo, M.; Thomas John, M. Single-Site Photocatalytic Solids for the Decomposition of Undesirable Molecules. *Chem. Commun.* **2006**, 3273−3278.
(77) Hwang, J.-S.; Chang, J.-S.; Park, S.-E.; Ikeue, K.; Anpo, M. Photoreduction of Carbon Dioxide on Surface Functionalized Nanoporous Catalysts. *Top. Catal.* **2005**, *35*, 311−319.
(78) Lin, W.; Han, H.; Frei, H. CO_2 Splitting by H_2O to CO and O_2 under UV Light in TiMCM-41 Silicate Sieve. *J. Phys. Chem. B* **2004**, *108*, 18269−18273.
(79) Matsuoka, M.; Anpo, M. Local structures, excited states, and photocatalytic reactivities of highly dispersed catalysts constructed within zeolites. *J. Photochem. Photobiol., C* **2003**, *3*, 225−252.
(80) Ikeue, K.; Nozaki, S.; Ogawa, M.; Anpo, M. Characterization of self-standing Ti-containing porous silica thin films and their reactivity for the photocatalytic reduction of CO_2 with H_2O. *Catal. Today* **2002**, *74*, 241−248.
(81) Ulagappan, N.; Frei, H. Mechanistic Study of CO_2 Photoreduction in Ti Silicalite Molecular Sieve by FT-IR Spectroscopy. *J. Phys. Chem. A* **2000**, *104*, 7834−7839.
(82) Anpo, M.; Yamashita, H.; Matsuoka, M.; Park, D. R.; Shul, Y. G.; Park, S. E. Design and development of titanium and vanadium oxide photocatalysts incorporated within zeolite cavities and their photocatalytic reactivities. *J. Ind. Eng. Chem.* **2000**, *6*, 59−71.
(83) Zhang, S. G.; Fujii, Y.; Yamashita, H.; Koyano, K.; Tatsumi, T.; Anpo, M. Photocatalytic reduction of CO_2 with H_2O on Ti-MCM-41 and Ti-MCM-48 mesoporous zeolites at 328 K. *Chem. Lett.* **1997**, 659−660.
(84) Ikeue, K.; Mukai, H.; Yamashita, H.; Inagaki, S.; Matsuoka, M.; Anpo, M. Characterization and photocatalytic reduction of CO_2 with H_2O on Ti/FSM-16 synthesized by various preparation methods. *J. Synchrotron Radiat.* **2001**, *8*, 640−642.
(85) Anpo, M.; Takeuchi, M. The design and development of highly reactive titanium oxide photocatalysts operating under visible light irradiation. *J. Catal.* **2003**, *216*, 505−516.
(86) Lin, W.; Frei, H. Bimetallic Redox Sites for Photochemical CO_2 Splitting in Mesoporous Silicate Sieve. *C. R. Chim.* **2006**, *9*, 207−213.
(87) Frei, H. Polynuclear Photocatalysts in Nanoporous Silica for Artificial Photosynthesis. *Chimia* **2009**, *63*, 721−730.
(88) Cuk, T.; Weare, W. W.; Frei, H. Unusually Long Lifetime of Excited Charge-Transfer State of All-Inorganic Binuclear $TiOMn^{II}$ Unit Anchored on Silica Nanopore Surface. *J. Phys. Chem. C* **2010**, *114*, 9167−9172.
(89) Lin, W.; Frei, H. Anchored Metal-to-Metal Charge-Transfer Chromophores in a Mesoporous Silicate Sieve for Visible-Light Activation of Titanium Centers. *J. Phys. Chem. B* **2005**, *109*, 4929−4935.
(90) Nakamura, R.; Frei, H. Visible Light-Driven Water Oxidation by Ir Oxide Clusters Coupled to Single Cr Centers in Mesoporous Silica. *J. Am. Chem. Soc.* **2006**, *128*, 10668−10669.
(91) Atienzar, P.; Valencia, S.; Corma, A.; Garcia, H. Titanium-containing zeolites and microporous molecular sieves as photovoltaic solar cells. *ChemPhysChem* **2007**, *8*, 1115−1119.
(92) Atienzar, P.; Navarro, M.; Corma, A.; Garcia, H. Photovoltaic activity of Ti/MCM-41. *ChemPhysChem* **2009**, *10*, 252−256.
(93) Kubacka, A.; Fernandez-Garcia, M.; Colon, G. Advanced Nanoarchitectures for Solar Photocatalytic Applications. *Chem. Rev.* **2012**, *112*, 1555−1614.
(94) Liu, G.; Wang, K.; Hoivik, N.; Jakobsen, H. Progress on free-standing and flow-through TiO_2 nanotube membranes. *Sol. Energy Mater. Sol. Cells* **2012**, *98*, 24−38.
(95) Su, Z.; Zhou, W. Formation, morphology control and applications of anodic TiO_2 nanotube arrays. *J. Mater. Chem.* **2011**, *21*, 8955−8970.
(96) Shankar, K.; Basham, J. I.; Allam, N. K.; Varghese, O.; Mor, G. K.; Feng, X.; Paulose, M.; Seabold, J. A.; Choi, K.-S.; Grimes, C. A. Recent Advances in the Use of TiO_2 Nanotube and Nanowire Arrays for Oxidative Photoelectrochemistry. *J. Phys. Chem. C* **2009**, *113*, 6327−6359.
(97) Natarajan, T. S.; Natarajan, K.; Bajaj, H. C.; Tayade, R. J. Energy Efficient UV-LED Source and TiO_2 Nanotube Array-Based Reactor for Photocatalytic Application. *Ind. Eng. Chem. Res.* **2011**, *50*, 7753−7762.
(98) Tachikawa, T.; Fujitsuka, M.; Majima, T. Mechanistic Insight into the TiO_2 Photocatalytic Reactions: Design of New Photocatalysts. *J. Phys. Chem. C* **2007**, *111*, 5259−5275.
(99) Aprile, C.; Corma, A.; Garcia, H. Enhancement of the photocatalytic activity of TiO_2 through spatial structuring and particle size control: From subnanometric to submillimetric length scale. *Phys. Chem. Chem. Phys.* **2008**, *10*, 769−783.
(100) Richter, C.; Schmuttenmaer, C. A. Exciton-like trap states limit electron mobility in TiO_2 nanotubes. *Nat. Nanotechnol.* **2010**, *5*, 769−772.

(101) Roy, P.; Kim, D.; Lee, K.; Spiecker, E.; Schmuki, P. TiO_2 nanotubes and their application in dye-sensitized solar cells. *Nanoscale* **2010**, *2*, 45−59.
(102) Roy, S. C.; Varghese, O. K.; Paulose, M.; Grimes, C. A. Toward Solar Fuels: Photocatalytic Conversion of Carbon Dioxide to Hydrocarbons. *ACS Nano* **2010**, *4*, 1259−1278.
(103) Mor, G. K.; Varghese, O. K.; Paulose, M.; Shankar, K.; Grimes, C. A. A review on highly ordered, vertically oriented TiO_2 nanotube arrays: Fabrication, material properties, and solar energy applications. *Sol. Energy Mater. Sol. Cells* **2006**, *90*, 2011−2075.
(104) Schulte, K. L.; De, S. P. A.; Gray, K. A. Effect of crystal phase composition on the reductive and oxidative abilities of TiO_2 nanotubes under UV and visible light. *Appl. Catal., B* **2010**, *97*, 354−360.
(105) Vijayan, B.; Dimitrijevic, N. M.; Rajh, T.; Gray, K. Effect of calcination temperature on the photocatalytic reduction and oxidation processes of hydrothermally synthesized titania nanotubes. *J. Phys. Chem. C* **2010**, *114*, 12994−13002.
(106) Varghese, O. K.; Paulose, M.; LaTempa, T. J.; Grimes, C. A. High-Rate Solar Photocatalytic Conversion of CO_2 and Water Vapor to Hydrocarbon Fuels. *Nano Lett.* **2009**, *9*, 731−737.
(107) Nazeeruddin, M. K.; De Angelis, F.; Fantacci, S.; Selloni, A.; Viscardi, G.; Liska, P.; Ito, S.; Takeru, B.; Grätzel, M. Combined experimental and DFT-TDDFT computational study of photoelectrochemical cell ruthenium sensitizers. *J. Am. Chem. Soc.* **2005**, *127*, 16835−16847.
(108) Zhu, K.; Neale, N. R.; Halverson, A. F.; Kim, J. Y.; Frank, A. J. Effects of Annealing Temperature on the Charge-Collection and Light-Harvesting Properties of TiO_2 Nanotube-Based Dye-Sensitized Solar Cells. *J. Phys. Chem. C* **2010**, *114*, 13433−13441.
(109) Park, J. H.; Kim, S.; Bard, A. J. Novel Carbon-Doped TiO_2 Nanotube Arrays with High Aspect Ratios for Efficient Solar Water Splitting. *Nano Lett.* **2006**, *6*, 24−28.
(110) Kim, J. C.; Choi, J.; Lee, Y. B.; Hong, J. H.; Lee, J. I.; Yang, J. W.; Lee, W. I.; Hur, N. H. Enhanced photocatalytic activity in composites of TiO_2 nanotubes and CdS nanoparticles. *Chem. Commun.* **2006**, 5024−5026.
(111) Lin, C.-J.; Lu, Y.-T.; Hsieh, C.-H.; Chien, S.-H. Surface modification of highly ordered TiO_2 nanotube arrays for efficient photoelectrocatalytic water splitting. *Appl. Phys. Lett.* **2009**, *94*, 113102/1−113102/3.
(112) Feng, X.; Sloppy, J. D.; LaTempa, T. J.; Paulose, M.; Komarneni, S.; Bao, N.; Grimes, C. A. Synthesis and deposition of ultrafine Pt nanoparticles within high aspect ratio TiO_2 nanotube arrays: Application to the photocatalytic reduction of carbon dioxide. *J. Mater. Chem.* **2011**, *21*, 13429−13433.
(113) Shao, W.; Gu, F.; Li, C.; Lu, M. Highly Efficient Dye-Sensitized Solar Cells by Using a Mesostructured Anatase TiO_2 Electrode with High Dye Loading Capacity. *Ind. Eng. Chem. Res.* **2010**, *49*, 9111−9116.
(114) Maeda, K.; Domen, K. Photocatalytic Water Splitting: Recent Progress and Future Challenges. *J. Phys. Chem. Lett.* **2010**, *1*, 2655−2661.
(115) Hernandez-Alonso, M. D.; Fresno, F.; Suarez, S.; Coronado, J. M. Development of alternative photocatalysts to TiO_2: Challenges and opportunities. *Energy Environ. Sci.* **2009**, *2*, 1231−1257.